JOURNAL OF CATALYSIS 142, 406–417 (1993)

The Partial Oxidation of Methane on MoO_3/SiO_2 Catalysts: Influence of the Molybdenum Content and Type of Oxidant

M. A. BAÑARES,* J. L. G. FIERRO,* AND J. B. MOFFAT†

Instituto de Catalisis y Petroleoquimica, 28006 Madrid, Spain; and †Department of Chemistry and the Guelph-Waterloo Centre for Graduate Work in Chemistry, University of Waterloo, Waterloo, Ontario, Canada N2L 3G1

Received November 3, 1992; revised March 17, 1993

The selective oxidation of methane to formaldehyde at atmospheric pressure was studied over a series of silica supported molybdena catalysts. Two silica supports of substantially different surface areas (80 and 200 m^2/g) and molybdenum contents ranging from 0 to 3.5 Mo/nm^2 were used for this purpose. The catalytic performance of the two catalyst series was compared for a wide range of experimental conditions, including the influence of the oxidant in the feed (O_2 or N_2O). The main products of the oxidation reaction were formaldehyde, CO and CO_2. Small amounts of C_2H_6 and CH_3OH were also identified. For typical reaction conditions, i.e., reaction temperatures 863 K, W/F = 4.5 g h/mol and CH_4/O_2 = 10 M both methane conversion and formaldehyde selectivity were higher with O_2 as oxidant. Furthermore, formaldehyde selectivity reached a maximum for molybdenum concentrations ca. 1 Mo/nm^2 with both oxidants. The molybdenum exposure on the surface of fresh and spent catalysts was monitored by X-ray photoelectron spectroscopy.

© 1993 Academic Press, Inc.

INTRODUCTION

While interest in the catalytic conversion of methane continues unabated, the focus of attention has gradually shifted from the partial oxidation process as pioneered by Lunsford and co-workers (*1*) and Somorjai and co-workers (*2*) to oxidative coupling originally researched by Keller and Bhasin (*3*). However, studies of the partial oxidation process offer interesting practical and fundamental aspects and as a consequence merit continued attention.

As Pitchai and Klier noted in their 1986 review, catalysts based on MoO_3 were the most widely studied for the partial oxidation of methanol at least up to that date (*4*). A more recent review by Brown and Parkyns (*5*) provides an updated summary demonstrating that the studies of this process have extended to include compounds of chromium, vanadium, iron, and tungsten. Other reviews appearing in the last several years include those of Garcia and Löffler (*6*), Foster (*7*), Gesser *et al.* (*8*), Scurrell (*9*), Mimoun (*10*), Sinev *et al.* (*11*), Anderson (*12*), and Lee and Oyama (*13*).

The report from Brown and Parkyns (*5*) emphasizes the importance of the direct process from methane to methanol in order to circumvent the route through syngas. However, as these authors emphasize the conversions and selectivities required to make the direct process economical have not yet been achieved.

Earlier work from one of our laboratories focused on the partial oxidation of methane over silica-supported metal-oxygen cluster catalysts containing one or more of molybdenum, tungsten, and vanadium (*14–27*). The effect of replacing the proton in these catalysts by larger cations was also evaluated (*21–24*). Comparisons with silica-supported molybdenum oxide were also reported (*14*). Later work provided evidence for the formation of metal-oxygen clusters such as 12-molybdosilicic acid from the interaction of MoO_3 with the silica support

0021-9517/93 $5.00
Copyright © 1993 by Academic Press, Inc.
All rights of reproduction in any form reserved.

(*22*). The production of oxidation products over the silica support itself has also been documented and the effect of the use of oxygen or nitrous oxide noted (*15*).

Most recently, Spencer and co-workers have reported that the partial oxidation of methane to formaldehyde by molecular oxygen is catalyzed by both MoO_3/SiO_2 and V_2O_5/SiO_2 (*28–32*). With the former catalyst methane is converted to H_2CO in parallel with CO_2, with the former product being further oxidized to CO, while with the latter catalyst a sequential mechanism appears to exist in which the CO_2 is formed from the CO. The most recent paper on this subject from these authors proposes a mechanism for the partial oxidation of methane on the two aforementioned catalysts (*32*). The same reaction was investigated by Kennedy *et al.* (*33*) over a range of silica-supported molybdena and vanadia catalysts promoted with silver, iron, chromium, cobalt, and sodium, but none of these additives assisted in the selective oxidation of methane to formaldehyde.

The present work examines the partial oxidation of methane over a series of MoO_3/SiO_2 with a variety of loadings of MoO_3, with two silica supports of substantially different surface areas and with two oxidants, nitrous oxide and oxygen.

EXPERIMENTAL

Two silica samples were employed in this work. One was an Aerosil MOX 80 (Degussa Iberica, S.A.) with surface area of 86 m^2/g and an Aerosil 200 of surface area 200 m^2/g (Table 1). Chemical composition and textural parameters for these silicas supports are summarized in Table 1.

The silica was impregnated with aqueous solutions of ammonium heptamolybdate (Merck) whose concentrations were selected to obtain surface concentrations up to 3.5 Mo atoms per nm^2. The two-phase system was dried in a rotary evaporator at 80°C and reduced pressure and then calcined in two steps: 2 h at 350°C and 4 h at 650°C. The catalysts supported on low and high surface area silica are referred to hereafter as Mox and 2Mox, respectively, where x denotes the surface concentration of Mo atoms per nm^2. The loadings and surface areas (BET) of the supported catalysts are shown in Table 2.

TABLE 1

Chemical Composition and Textural Properties of the Silica Supports

Support: Source:	Aerosil MOX-80 Degussa	Aerosil 200 Degussa
Composition (wt%)		
SiO_2:	>98.3	>99.8
Al_2O_3:	0.3–1.3	<0.05
Fe_2O_3:	<0.01	<0.003
TiO_2:	<0.02	<0.03
Na(ppm):	<450	—
HCl:	<0.025	<0.025
Average particle size (nm):	30	12
Surface area (m^2/g):	80 ± 20	200 ± 25

The catalytic reactions employed a quartz reactor with either nitrous oxide or oxygen as oxidant, CH_4/oxidant molar ratios from 11/1 to 4.5/1 and W/F between 1.5 and 7.0 g h mol^{-1}. Except where otherwise indicated 200 mg of the catalyst was employed. The reactor system was equipped with an on-line gas chromatograph (Shimadzu GC-9A, when working with N_2O and Konik-3000HR when working with O_2) fitted with a 10′ × $\frac{1}{8}$″ Porapak-Q column and a 4A molecular sieve column. Calibrations for formaldehyde were obtained with a 37% HCHO aqueous solution stabilized with 10% CH_3OH. A suitable temperature was employed for the former column and 35°C for the latter. The catalyst was heated in the reactor under an oxygen flow from 25 to 200°C and held at the latter temperature for approximately 2 h. The temperature was subsequently increased to the reaction temperature. Approximately 2 h were required to reach apparently steady conditions. Sampling of the products stream was repeated until the analytical results were reproduc-

TABLE 2

Molybdena Loadings and BET Areas of the Supported Catalysts

Aerosil MOX-80				Aerosil-200			
Label	MoO_3 (wt%)	Surface area (m^2/g)	MoO_3^a/ nm^2	Label	MoO_3 (wt%)	Surface area (m^2/g)	MoO_3^a/nm^2
Mo 0.3	0.5	76.7	0.3	2Mo 0.3	0.5	182.7	0.3
Mo 0.4	0.8	69.3	0.4	2Mo 0.5	1.1	166.2	0.5
Mo 0.6	1.1	67.7	0.6	2Mo 0.8	1.7	160.2	0.8
Mo 1.0	1.7	69.3	1.0	2Mo 1.3	3.5	114.1	1.3
Mo 1.5	2.5	79.9	1.5	2Mo 1.9	6.7	69.0	1.9
Mo 1.9	3.5	40.1	1.9	2Mo 3.5	16.2	23.6	3.5
Mo 2.7	4.6	43.7	2.7				
Mo 3.5	6.7	55.7	3.5				

[a] Number of molecules per nm^2 of support assuming 100% dispersion.

ible. To evaluate the formation of H_2, parallel analysis of the permanent gases was carried out in an HP5890A gas chromatograph with a 10′ × ⅛″ Chromosorb 107 and using Ar as a carrier.

X-ray photoelectron spectra were obtained with a Fisons ESCALAB 200R spectrometer interfaced to a data station and fitted with a hemispherical electron analyzer and a magnesium X-ray source (Mg$K\alpha$ = 1253.6 eV). The samples were outgassed at room temperature to 5×10^{-5} Torr in a prechamber prior to being transferred into the analysis chamber. The pressure in the latter was maintained at less than 4×10^{-9} Torr during analysis. The spectra were recorded in 20-eV-wide regions centred at the relevant energies and at a pass energy of 20 eV. Each spectral region was signal-averaged to a number of scans to obtain good signal/noise ratios. Although surface charging was observed in all samples, accurate binding energies (BE) were calculated by referencing to the Si 2p line at 103.4 eV.

RESULTS

Blank Experiments

The conversion of methane on silica and in homogeneous gas-phase reactions was investigated. For a feed ratio of CH_4/O_2 equal to 11, the gas-phase reaction was found to occur only to a very small extent at the highest reaction temperature (630°C) with trace amounts of C_2H_6 detected in the reactor exit stream. Blank experiments with the Aerosil 200 carrier were also performed in the temperature range 550–630°C with feed ratios of CH_4/O_2 equal to 11 and methane residence time of 4.5 g h/mol. The conversion of methane was found to be extremely low at temperatures below 600°C, with traces of carbon oxides and HCHO being the only detectable carbon-containing compounds. At higher temperatures the conversion of methane increased slightly up to levels of the order of 0.1% but only carbon oxides were detected.

XPS Results

The Mo 3d and Si 2p core-level spectra were recorded for both fresh and used catalysts. The binding energies of the most intense Mo $3d_{5/2}$ peak are tabulated in Table 3. The values range from 232.2 to 233.0 eV. Since no systematic changes are evident, it can be concluded that neither changes in loading nor use of the catalyst alter the position of the Mo $3d_{5/2}$ peak. A common feature to all these spectra is the poor resolution of the Mo 3d doublet irrespective of the Mo-loading, which indicates the formation of some reduced molybdenum oxides by X-ray irradiation during analysis.

TABLE 3

Binding Energies for Mo $3d_{5/2}$ Peak for MoO_3/SiO_2 Catalysts at Various Loadings on a Low- and a High-Surface-Area Support

Catalyst	S_{BET} (m^2/g)	Mo $3d_{5/2}$ (eV)		
		Fresh	O_2-used	N_2O-used
Mo 0.3	77	233.0	232.8	—
Mo 0.4	69	232.4	232.5	232.6
Mo 0.6	68	233.0	232.3	232.6
Mo 1.0	69	232.9	232.6	232.5
Mo 1.5	65	232.8	232.5	232.8
Mo 1.9	40	233.0	232.9	232.7
Mo 2.7	44	233.0	232.7	232.6
Mo 3.5	42	232.6	232.6	232.7
2Mo 0.3	183	232.5	232.2	232.4
2Mo 0.5	166	232.6	232.5	232.5
2Mo 0.8	161	232.7	232.5	232.3
2Mo 1.3	114	232.4	232.6	232.6
2Mo 1.9	69	232.6	232.4	232.4
2Mo 3.5	24	232.8	232.6	232.6

The intensity of Mo $3d$ peaks relative to that of the Si $2p$ in the support as calculated from the XPS data for the catalysts both new and used shows the expected trends with loading except for the higher area supports with relatively high loading (Table 4). As a consequence of the relatively large variation in measured surface areas for a given support, the differences between molybdenum concentrations as prepared and as measured, vary considerably. It is particularly interesting to note that the I_{Mo}/I_{Si} values for the used catalysts are higher than those for the new catalysts for all loadings and both supports. In particular, catalysts with N_2O as oxidant showed a wide full width at half maxima of the Mo $3d$ doublet, which suggests the presence of reduced Mo-species in these catalysts.

TABLE 4

XPS Relative Intensities of Fresh and Used Catalysts at Various Loadings on a Low- and a High-Surface-Area Support

Catalyst	S_{BET} (m^2/g)	I_{Mo}/I_{Si}		
		Fresh	O_2-used	N_2O-used
Mo 0.3	77	0.0397	0.0530	—
Mo 0.4	69	0.0533	0.0670	0.0517
Mo 0.6	68	0.0871	0.1124	0.2279
Mo 1.0	69	0.0941	0.1850	0.1067
Mo 1.5	65	0.1864	0.1882	0.2305
Mo 1.9	40	0.3174	0.3760	0.2968
Mo 2.7	44	0.4890	0.5208	0.3898
Mo 3.5	42	0.2944	0.4080	0.4440
2Mo 0.3	183	0.0338	0.0324	0.0510
2Mo 0.5	166	0.0687	0.0653	0.0796
2Mo 0.8	161	0.0786	0.0997	0.1195
2Mo 1.3	114	0.1732	0.3500	0.1761
2Mo 1.9	69	0.1620	0.1344	0.2620
2Mo 3.5	24	0.4770	0.4473	0.3371

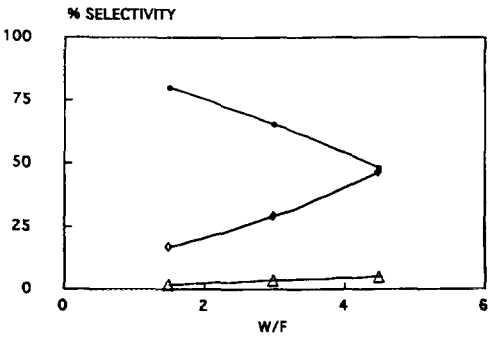

FIG. 1. Influence of contact time on product distribution for the catalyst Mo 0.6: (●) HCHO, (◇) CO, and (△) CO_2. CH_4/O_2 = 11, reaction temperature, 590°C.

Activity Results

Oxygen as oxidant. With either nitrous oxide or oxygen, the products of the reaction are predominantly CO, CO_2, and HCHO with, in some cases, ethane and methanol. Molar balances on the carbon and oxygen were 1.00 ± 0.01 and 1.00 ± 0.05, respectively. It has been observed that either an increase of methane residence time or of the reaction temperature is reflected in an increase of the methane and oxygen conversions. The product distributions are affected in the sense that increasing conversion levels of CH_4 are followed by decreasing selectivity to HCHO with a concurrent increase in the selectivity to CO, while that to CO_2 is largely unchanged. This trend is illustrated in Fig. 1 for the catalyst Mo 0.6.

TABLE 5

Effect of the Reaction Temperature on the Oxidation of CH_4 with O_2

Temperature (K)	% Conversion		% Selectivity (*M*)				
	CH_4	O_2	CO	CO_2	C_2H_6	HCHO	CH_3OH
843	0.6	7.0	2.2	4.0	—	93.8	—
863	1.2	13.9	12.0	5.6	—	82.4	0.1
883	2.2	27.8	26.2	8.6	0.4	64.7	0.1

Note. Catalyst Mo 1.0; W/F = 4.5 g h/mol; CH_4/O_2 = 10 M.

Upon increasing W/F, the HCHO selectivity decreases markedly while that of CO increases; only a slight increase of CO_2 is observed. This indicates that HCHO is a primary product that decomposes to CO. The origin of CO_2 is much more complex. It may be produced directly from CH_4 as results at methane conversions as low as 0.6% have shown (Table 5). Similar findings have already been reported by Spencer and Pereira (*28*) for the selective oxidation of methane on catalysts with comparable molybdenum loadings. Recent work carried out in one of our laboratories using isotopic labelling techniques indicated that CO_2 comes directly from the interaction of methane with molybdena (*34*). It can be seen that more than one oxidation site is formed on the supported molybdenum oxide phase. With C_4 oxidation Ozkan *et al.* (*35*) suggested that molybdena has two oxidation sites: (i) complete oxidation, associated with Mo–O–Mo sites, and (ii) selective oxidation, thought to be associated with terminal oxygen sites (Mo=O). CO_2 may not only be produced directly from methane but also from the oxidation of CO or the water–gas shift (WGS) reaction of CO. In fact, according to the amounts of H_2 detected, ca. $\frac{1}{5}$ of the CO_2 observed probably originates from the WGS reaction. Even when the lattice oxygen of molybdena is incorporated in the methane molecule, some kind of activated adsorbed oxygen, which operates through a suprafacial mechanism, will be responsible for the nonselective oxidation of methane to carbon monoxide (*34*). However, the extent of this reaction appears to be unimportant since the close link between CO and HCHO suggests that the latter is the main source of CO. Moreover the competitive adsorption of CO_2 will decrease this possibility (*36*). As a whole, the picture of the reaction is that lattice oxygen will yield selective and complete oxidation products while gas phase molecular oxygen will be responsible for the non-selective oxidation of CH_4 to CO (Fig. 2).

At a reaction temperature of 590°C, CH_4/O_2 = 11 M and W/F = 4.5 g h/mol the conversions of methane and the yield to formaldehyde increase with molybdenum loading on the two catalyst series, pass through a maximum at intermediate loadings and then decrease at higher loadings (Figs. 3a and 3b). It is noteworthy that the maximum appears on the two catalyst series at an apparent surface density of approximately 1 Mo/nm^2, although the maximum

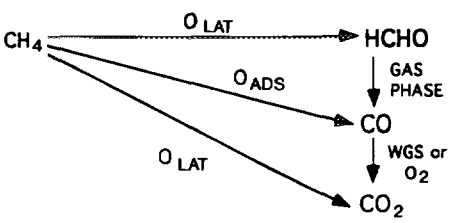

FIG. 2. Reaction pathway for the selective oxidation of methane over MoO_3/SiO_2 catalysts.

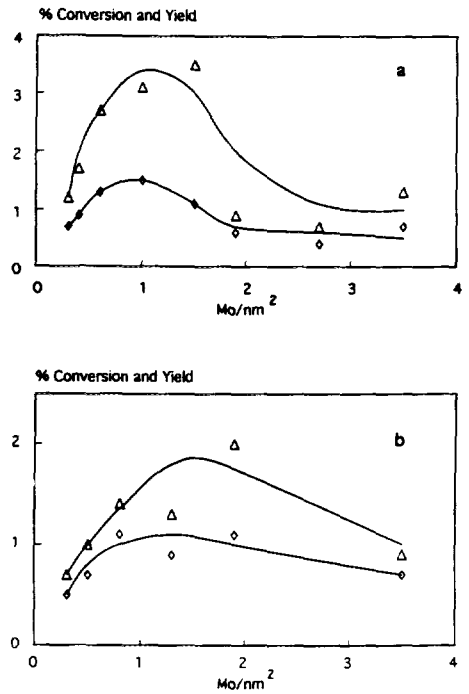

FIG. 3. Conversion of methane and yield of formaldehyde on MoO_3 supported on (a) Mox series and (b) 2Mox series. Reaction temperature 590°C; W/F = 4.5 g h/mol; CH_4/O_2 = 11 molar.

with the lower area support is more pronounced. However, the conversion of the catalysts prepared from the lower area supports achieves maximum values approximately twice as large as those obtained with the higher area silica.

At methane conversions of 1.0% and under the same reaction conditions the selectivities to formaldehyde also show a maximum with either support (Figs. 4a and 4b) but the values of the selectivity at the maximum are similar for both Mox and 2Mox catalyst series. The selectivities to the various products at 1.0% conversion of methane, 590°C and CH_4/O_2 = 11 are tabulated in Table 6 for the two catalyst series. It is evident that the increase in selectivity to formaldehyde with increasing loading is primarily at the expense of carbon dioxide with the lower surface area support but with concurrent decrease in the selectivity to CO on the higher surface area support.

Oxidation with nitrous oxide. The selective oxidation of methane with nitrous oxide also yielded CO, HCHO, and CO_2 as the principal products. The trends in the conversions and product distributions with increasing reaction temperature or methane residence time in the bed of the catalyst are the same as those observed with molecular oxygen. However, there are significant differences in both activity and selectivity. Not only the methane and oxidant conversions are significantly lower, but also at the same level of methane conversion and reaction temperature HCHO selectivity is much lower than that in the presence of molecular oxygen (Figs. 5a and 5b).

In addition, the effect of the molybdenum loading on the catalytic performance in the reaction using N_2O as oxidant (Fig. 6) fol-

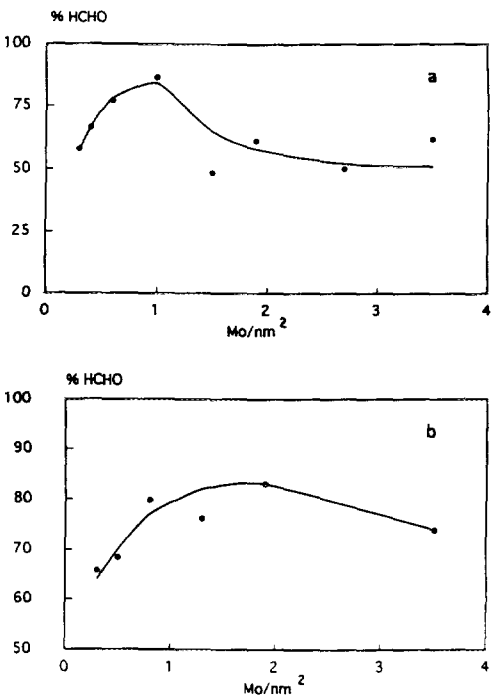

FIG. 4. Selectivities to formaldehyde on (a) Mox series and (b) 2Mox series. Conversion of methane 1.0%; reaction temperature 590°C; CH_4/O_2 = 11 molar.

TABLE 6

Product Distribution at 1.0% CH_4 Conversion on the Two Catalyst Series

Catalyst	% Selectivity (*M*)				
	CO	CO_2	C_2H_6	HCHO	CH_3OH
		Low surface area			
Mo 0.3	23.7	16.5	1.0	57.9	0.2
Mo 0.4	27.4	3.4	1.2	66.4	0.3
Mo 0.6	19.2	1.9	0.8	77.0	0.2
Mo 1.0	8.5	5.0	—	86.4	0.1
Mo 1.5	46.7	4.2	0.5	48.5	—
Mo 1.9	33.1	5.5	—	61.3	—
Mo 2.7	42.4	7.4	—	50.1	—
Mo 3.5	34.8	3.3	—	61.8	—
		High surface area			
2Mo 0.3	24.8	4.3	4.6	65.8	0.4
2Mo 0.5	22.7	8.6	0.2	68.4	t
2Mo 0.8	15.5	4.6	—	79.8	t
2Mo 1.3	18.7	5.1	—	76.2	t
2Mo 1.9	14.9	1.7	—	83.0	—
2Mo 3.5	21.2	4.9	—	73.8	—

Note. T = 590°C and CH_4/O_2 = 11.

lowed almost the same profile as that with molecular oxygen. The two profiles for Mox and 2Mox catalysts series display a maximum in methane conversion for loadings close to 1.0 Mo/nm^2.

DISCUSSION

Effect of Molybdenum Loading

The catalytic activity data for the selective oxidation of methane with molecular oxygen on Mox and 2Mox catalysts series show a clear dependence on the molybdenum content. The characterization of the catalysts by Raman, XPS, and XRD reveals that molybdenum loading determines the nature of the supported species. Some information about the mode of distribution of the various molybdenum species can also be derived from the analysis of the ensemble of data.

The almost linear dependence of the normalized XPS Mo/Si intensity ratios (Fig. 7) on molybdenum concentrations up to about 1.0 and 2.5 Mo/nm^2 in the two Mox and 2Mox series, respectively, indicates that molybdenum species were distributed uniformly on the silica surface. The loss of resolution of the Mo 3*d* doublet in this concentration range as compared with that in bulk MoO_3 and the progressive decrease in surface area, particularly in the 2Mox series, indicate that the supported molybdenum oxide phase interacted strongly with the silica

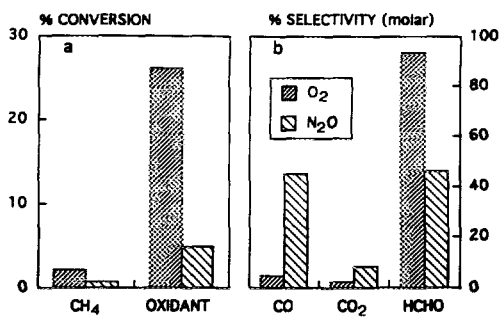

FIG. 5. (a) Conversions of methane and oxidant for the Mo 0.6 catalyst at W/F = 4.5 g h/mol and T = 863 K. CH_4/O_2 = 11 M and CH_4/N_2O = 5 M. (b) Product distribution at methane conversion of 0.6% and T = 863 K.

surface. Surface molybdate species may be identified through the use of the Raman data reported earlier (*37*). For molybdenum concentrations of 0.8 Mo/nm^2 only a weak band at ca. 960 cm^{-1} was observed which may be attributed to a highly dispersed molybdate species previously proposed by Jeziorowsky and Knözinger (*38*), Stencel *et al.* (*39*), and Wachs and co-workers (*40*) for similar catalysts prepared by a variety of methods. At molybdenum concentrations above 0.8 Mo/nm^2 the Raman spectra are dominated by the bands of MoO_3 crystalline structures, but these results do not exclude the simultaneous presence of polymolybdates and MoO_3 crystallites. In this point it must be noted that the latter are good Raman scatterers while the former are poor scatterers since they are heterogeneously distributed on the surface (*41*). The appearance of an XRD pattern of crystalline MoO_3 and the decrease of the XPS Mo/Si ratios in this concentration range (*42*), particularly for the 2Mo*x* catalyst series, are also consistent with that observation.

In a previous study using labelling techniques we have shown that only lattice oxygen of molybdenum oxide in MoO_3/SiO_2 catalysts is responsible for the selective oxidation of methane to formaldehyde (*34*). Judging from the data of Fig. 3, and particularly of Fig. 6, one would infer that the

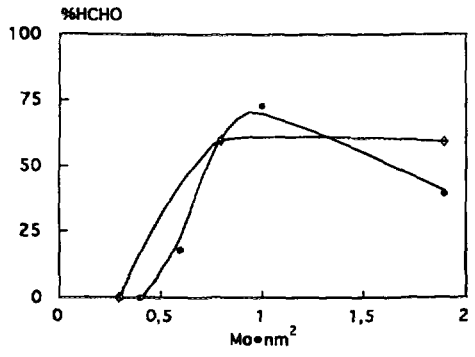

FIG. 6. HCHO selectivity at 863 K for CH_4 conversion of 0.2% and CH_4/N_2O = 5 M for catalysts of Mo*x* series (●) and of 2Mo*x* series (◇).

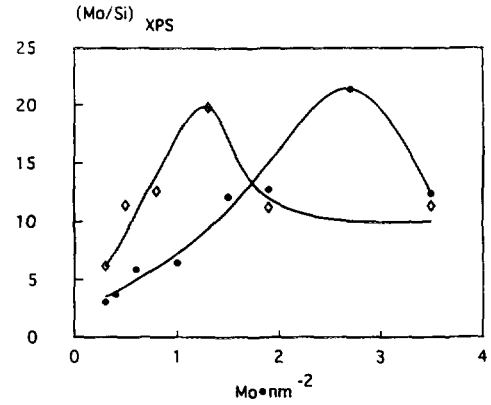

FIG. 7. Dependence of Mo concentration of the XPS Mo/Si intensity ratios for Mo*x* (◇) and 2Mo*x* (●) catalyst series.

HCHO selectivity is directly related to dispersed molybdate structures in these catalysts. It can be noted in these figures that HCHO selectivity increases gradually with molybdenum concentration up to 0.8 Mo/nm^2 for the two catalysts series when molecular oxygen is used as an oxidant (Fig. 4), however, the increase is much more marked in that region of compositions when N_2O is fed into the reactor. As discussed below, although these differences may reside in the inability of N_2O to restore a given oxidation state of molybdenum, there is a common feature, that is, the best HCHO selectivity is obtained in the composition range where polymolybdates are developed. It is presumed that the binding energy of oxygen in these structures attains values which make these selective. In line with this interpretation one would expect that molybdena dispersion is not related to HCHO selectivity. To verify this, HCHO selectivities have been plotted against normalized I_{Mo}/I_{Si} in Fig. 8. Although some variation of the selectivity to HCHO with the XPS I_{Mo}/I_{Si} ratio is evident, particularly for the Mo*x* series of catalysts, nevertheless the data in Fig. 8 suggest that the molybdate species are developed at very low molybdenum concentrations and these are preserved on the catalyst surface as the molybdenum loading increases.

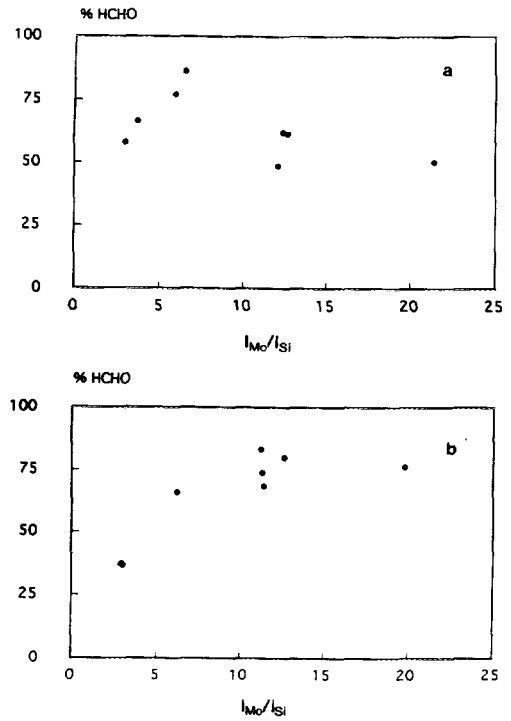

FIG. 8. Dependence of HCHO selectivity at 590°C, W/F = 4.5 g h/mol and CH_4/O_2 = 11 M on the XPS Mo/Si intensity ratios for (a) Mox series and (b) 2Mox series.

The smoother profiles observed in the catalytic activity of the 2Mox catalysts series with respect to its Mox counterpart as a function of the molybdenum loading can be due to the smaller size of the silica microspheres (12 nm versus 30 nm diameter) that will favour the larger participation of aggregates from lower apparent surface molybdenum densities. This will give a more uniform behaviour of the series as the change in the nature of molybdenum species will be smaller.

It is of interest to compare the present results on the effect of loading with those obtained earlier in one of our laboratories for the 12-molybdophosphoric acid/SiO_2 system (*14–18*, *21–24*), particularly since there appear to be some interesting similarities between the results for the two catalytic systems. With 12-molybdophosphoric acid supported on silica (abbreviated to HPMo/SiO_2) conversion increased linearly to a maximum at approximately 20 wt% HPMo on SiO_2. This corresponds to a coverage of approximately one anion per 10 nm^2 as compared with the value of 1 nm^2 estimated for the cross-sectional area of an anion of HPMo. In addition the XPS Mo_{3d}/Si_{2p} intensity ratio was found to be approximately linear up to a HPMo loading of approximately 0.1 anion/nm^2 again, as in the present work indicating a uniform distribution of the supported species on the surface. Finally the earlier studies of MoO_3/SiO_2 provided Raman spectra showing the formation of molybdosilicic acid (*22*). However it is apparent that the generation of such species on the surface of the silica is undoubtedly favoured by an acidic environment. Although a semiquantitative correspondence between these earlier results on HPMo/SiO_2 and the present data is evident, it is important to note that no evidence for the formation of molybdosilicic acid has been found in the present work.

Effect of the Oxidant

It is generally believed that the selective oxidation of methane on redox catalysts occurs via a Mars–van Krevelen mechanism in which the catalyst is alternately reduced by methane and reoxidized by the gaseous oxidant. Such a mechanism has been already confirmed by a tracer isotopic technique which demonstrated that the oxygen of HCHO comes directly from the molybdenum oxide lattice (*34*). Apart from this, there is no general consensus on the type of oxygen species responsible for the reaction. Thus, Barbaux *et al.* (*43*) pointed out that oxidation of methane with molecular oxygen on bulk and low Mo-content catalysts occurs via O^- species, carbon monoxide and carbon dioxide being only reaction products. Conversely, when nitrous oxide was used as an oxidizing agent, the type of oxygen species which participated in the reaction depended on the type of catalyst. Par-

ticularly, at low Mo-loadings, the O^{2-} species were involved in methane oxidation; however, on bulk MoO_3, on which only combustion was observed, the O^- species were shown to be active in the reaction. The work of Liu *et al.* (*44*) proposed, however, that both O^- and O^{2-} species are active: the former in the activation of methane to yield methyl radicals, and the latter in further oxidation of these radicals into formaldehyde.

The use of nitrous oxide instead of molecular oxygen is reflected in a lower methane conversion and formaldehyde selectivity. As the oxygen selectively incorporated in the methane comes from the lattice of molybdenum oxide and the role of the oxidant is to regenerate the oxide, the catalytic differences between these two systems may well arise from the different oxidizing power of N_2O and O_2. Accordingly, the reoxidation of the catalyst should be less effective in the presence of nitrous oxide. In favour of this interpretation is also the colour of the catalyst after reaction, which is light yellow or white after reaction with O_2 and presents an intense dark blue colour after reaction with N_2O, a colour which is characteristic of partially reduced molybdenum oxide (*45*). Also, the X-ray diffraction patterns reveal the presence of MoO_2 in the supported molybdenum after reaction under the latter conditions (Fig. 9) and the XP spectra showed a decrease in the resolution of the Mo 3*d* doublet with an increase in the full width at half maxima which suggests an overlapping in that energy region of Mo(VI) and Mo(IV) photoelectrons (Fig. 10). All these findings indicate that the average oxidation level in the supported molybdenum oxide is lower in the presence of N_2O than in molecular oxygen, thus limiting to some extent the availability of lattice oxygen for the selective oxidation.

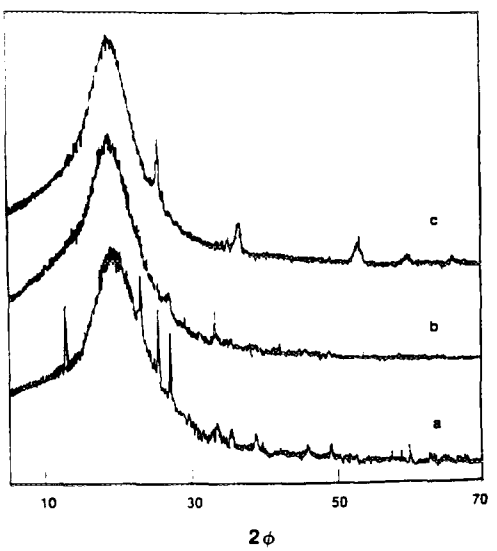

FIG. 9. X-ray diffraction patterns (λ = 0.1541 nm) of the 2Mo 1.9 catalyst: (a) fresh, (b) used with O_2 as oxidant, and (c) used with N_2O as oxidant.

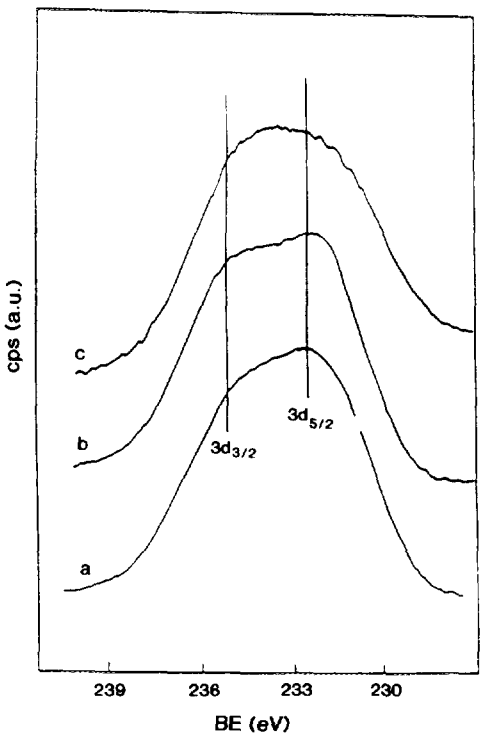

FIG. 10. XP spectra of Mo 3*d* level in catalyst 2Mo 1.9: (a) fresh, (b) after reaction in O_2, and (c) after reaction in N_2O.

CONCLUSIONS

Silica-supported molybdenum oxide is active in the selective oxidation with oxygen

of methane to formaldehyde, which is a primary product that decomposes to CO. The carbon dioxide will come from the subsequent water–gas shift reaction of CO or, most likely, directly from methane reacting with molybdenum oxide. The molybdenum loadings close to the limit of dispersion present the kind of molybdenum oxide species most effective in the selective oxidation and correspond to the identification of polymolybdates by laser Raman spectroscopy. Nitrous oxide appears to be less effective than oxygen to regenerate the catalyst during operation in a redox cycle.

ACKNOWLEDGMENTS

The financial support of the Natural Sciences and Engineering Research Council of Canada is gratefully acknowledged.

REFERENCES

1. Liu, H. F., Liu, R. S., Liew, K. Y., Johnson, R. E., and Lunsford, J. H., *J. Am. Chem. Soc.* **106,** 4117 (1984).
2. Khan, M. M., and Somorjai, G. A., *J. Catal.* **91,** 263 (1985); Zhen, K. J., Khan, M. M., Mak, C. H., Lewis, K. B., and Somorjai, G. A., *J. Catal.* **94,** 501 (1985).
3. Keller, G. E., and Bhasin, M. M., *J. Catal.* **73,** 9 (1982).
4. Pitchai, K., and Klier, K., *Catal. Rev. Sci. Eng.* **28,** 13 (1986).
5. Brown, M. J., and Parkyns, N. D., *Catal. Today* **8,** 305 (1991).
6. Garcia, E. Y., and Löffler, D. G., *Rev. Latinoam. Ing. Quim. Quim. Apl.* **14,** 267 (1986).
7. Foster, N. R., *Appl. Catal.* **19,** 1 (1985).
8. Gesser, H. D., Hunter, N. R., and Prakash, C. B., *Chem. Rev.* **85,** 235 (1985).
9. Scurrell, M. S., *Appl. Catal.* **32,** 1 (1987).
10. Mimoun, H., *New J. Chem.* **11,** 513 (1987).
11. Sinev, M. Yu., Korshak, V. N., and Krylov, O. V., *Russ. Chem. Rev.* **58,** 22 (1989).
12. Anderson, J. R., *Appl. Catal.* **47,** 177 (1989).
13. Lee, J. S., and Oyama, S. T., *Catal. Rev.-Sci. Eng.* **30,** 249 (1988).
14. Kasztelan, S., and Moffat, J. B., *J. Catal.* **106,** 512 (1987).
15. Kasztelan, S., and Moffat, J. B., *J. Chem. Soc. Chem. Commun.,* 1663 (1987).
16. Moffat, J. B., *in* "Keynotes in Energy-Related Catalysis" (S. Kaliaguine, Ed.), Studies in Surface Science and Catalysis, Vol. 35, p. 139. Elsevier, Amsterdam, 1988.
17. Moffat, J. B., *in* "Methane Conversion" (D. M. Bibby, C. D. Chang, and R. F. Howe, Eds.), Studies in Surface Science and Catalysis, Vol. 36, p. 563. Elsevier, Amsterdam, 1988.
18. Kasztelan, S., and Moffat, J. B., *J. Catal.* **109,** 206 (1988).
19. Ahmed, S., and Moffat, J. B., *Appl. Catal.* **40,** 101 (1988).
20. Ahmed, S., and Moffat, J. B., *Catal. Lett.* **1,** 141 (1988).
21. Kasztelan, S., and Moffat, J. B., *J. Catal.* **112,** 54 (1988).
22. Kasztelan, S., Payen, E., and Moffat, J. B., *J. Catal.* **112,** 320 (1988).
23. Kasztelan, S., and Moffat, J. B., *in* "Proceedings 9th International Congress on Catalysis, Calgary, 1988" (M. J. Phillips and M. Ternan, Eds.). Chemical Institute of Canada, Ottawa, 1988.
24. Kasztelan, S., and Moffat, J. B., *J. Catal.* **116,** 82 (1989).
25. Ahmed, S., and Moffat, J. B., *J. Phys. Chem.* **93,** 2542 (1989).
26. Ahmed, S., and Moffat, J. B., *J. Catal.* **118,** 281 (1989).
27. Ahmed, S., Kasztelan, S., and Moffat, J. B., *J. Chem. Soc. Faraday Discuss.* **87** (1989).
28. Spencer, N. D., and Pereira, C. J., *AIChE. J.* **33,** 1808 (1987).
29. Spencer, N. D., *J. Catal.* **109,** 187 (1988).
30. Spencer, N. D., and Pereira, C. J., *J. Catal.* **116,** 399 (1989).
31. Spencer, N. D., Pereira, C. J., and Grasselli, R. K., *J. Catal.* **126,** 546 (1990).
32. Amiridis, M. D., Rekoske, J. E., Dumesic, J. A., Rudd, D. F., Spencer, N. D., and Pereira, C. J., *AIChE J.* **37,** 87 (1991).
33. Kennedy, M., Sexton, A., Kartheuser, B., Mac Giolla Coda, E., McMonagle, J. B., and Hodnett, K. B., *Catal. Today* **13,** 447 (1992).
34. Bañares, M. A., Rodríguez-Ramos, I., Guerrero-Ruiz, A., and Fierro, J. L. G., *in* "Proceedings, 10th International Congress on Catalysis, Budapest, 1992," paper 076, p. 184. Elsevier, Amsterdam, 1993.
35. Ozkan, U. S., Smith, M. R., and Driscoll, S. A. "New Developments in Selective Oxidation," Louvain-la-Neuve, 1991.
36. Koranne, M. M., Goodwin Jr., J. G., and Marcelin, G., 10th International Congress on Catalysis, Budapest, 1992, paper O5, p. 14.
37. Bañares, M. A., and Fierro, J. L. G., *Prep. Am. Chem. Soc. Symp. Ser.* **37,** 1171 (1992).
38. Jeziorowski, H., and Knözinger, H., *J. Phys. Chem.* **30,** 471 (1975).
39. Stencel, J. M., Diehl, J. R., D'Este, J. R., Makovsky, L. E., Rodrigo, L., Marcinkowska, K., Adnot, A., Roberge, P. C., and Kaliaguine, S., *J. Phys. Chem.* **90,** 4739 (1983).
40. Kim, D. S., Segawa, K., Soeya T., and Wachs, I. E., *J. Catal.* **136,** 539 (1992).
41. Morrow, B. A. *in* "Spectroscopic Characteriza-

tion of Heterogenous Catalysts. Part A. Methods of Surface Analysis" (J. L. G. Fierro, Ed.), Vol. 57A, p. A161. Elsevier, Amsterdam, 1990.

42. Bañares, M. A. and Fierro, J. L. G., *in* "Proceedings XIII Iberoamerican Symposium on Catalysis, Segovia, 1992," p. 55.
43. Barbaux, Y., Elamrani, A. and Bonnelle, J. P., *Catal. Today* **1,** 147 (1987).
44. Liu, H. F., Liu, R. S., Liew, K. Y., Johnson, R. E. and Lunsford, J. H., *J. Am. Chem. Soc.* **106,** 501 (1984).
45. Kihlborg, L., *Acta Chem. Scand.* **16,** 2458 (1962).